Coplanar Stripline Resonators Modeling and Applications to Filters

Young-Ho Suh, *Student Member, IEEE,* and Kai Chang, *Fellow, IEEE*

***Abstract*—This paper presents coplanar stripline (CPS) resonators and their practical implementations to filters. Five types of CPS resonator are built using open- and short-ended strips. Lumped-element equivalent circuits are presented for each resonator. Their performances are investigated and compared in terms of Q factor or bandwidth. Two types of bandpass filter are developed with the resonators. The bandpass filters have low-passband insertion losses and wide-stopband suppression bandwidths. Lumped-element equivalent circuits are presented for the bandpass filters. A wide-band CPS-to-microstrip transition is developed for the measurements. The back-to-back transition has an insertion loss of less than 3 dB and a return loss of better than 10 dB for the frequency range from 1.3 to 13.3 GHz (1 : 10.2).**

***Index Terms*—Balun, coplanar stripline, coplanar-stripline bandpass filter, coplanar-stripline resonator, CPS-to-microstrip transition, equivalent circuit, Q factor, uniplanar bandpass filter, uniplanar resonator.**

I. Introduction

COPLANAR stripline (CPS) is an attractive uniplanar transmission line for solid-state device integration. Its balanced structure is useful in applications such as printed dipole antenna feeding [1], rectennas [2]–[4], uniplanar mixers [5], and opto-electric devices [6]. CPS characteristics are good propagation, small dispersion, small discontinuity parasitics, comparably insensitive to substrate thickness, and simple implementation of open- or short-ended strips. However, relatively little research has been done on CPS, as compared with coplanar waveguide (CPW). In 1993, characteristics of symmetric and asymmetric CPSs were investigated and analytic closed-form formulas were obtained using the conformal mapping for the quasi-TEM parameters [7]. More CPS studies regarding CPS on multilayer substrate [8] and computer-aided design (CAD) models for various CPS configurations [9] were conducted. In 1996, CPS discontinuities such as open and short circuits, series gap, spur slot, and spur strip were investigated [10]. In 1997, CPS discontinuities and their applications to bandstop [11] and bandpass [12] filters were studied by using the spur–strip and the spur–slot resonators. A lumped-element CPS low-pass filter was designed in 1998 [13], and a CPS low-pass filter using a transverse slit and a parallel-coupled gap of CPS discontinuities was presented in 1999 [14].

Manuscript received December 5, 2000. This work was supported in part by the National Aeronautics and Space Administration Marshall Space Flight Center.

The authors are with the Department of Electrical Engineering, Texas A&M University, College Station, TX 77843-3128 USA (e-mail: ysuh@ee.tamu.edu; chang@ee.tamu.edu).

Publisher Item Identifier S 0018-9480(02)04065-6.

Extensive work has been reported in CPW resonators and filters. Dib *et al.* investigated CPW discontinuities based on the solution of an appropriate surface integral equation in space domain in 1991 [15]. In [16], various types of CPW series resonators and their applications to filters were presented. In 1999, CPW shunt stubs printed within the center conductor were presented and miniature filters were implemented with the shunt stubs [17].

However, CPW shunt-stub resonator requires additional air bridges, which might increase the fabrication cost and complexity. CPW series resonators require large conductor area. The structure of CPW bandpass filter using CPW series resonators is comparably complex. Applications such as rectenna circuits require a uniplanar transmission line with high characteristic impedance for high RF-to-dc conversion efficiency of the detector diode [2]–[4]. CPS is the most proper transmission line for the rectenna application among other uniplanar transmission lines.

In this paper, five types of a CPS resonator are modeled and their performances are analyzed in terms of Q factor or bandwidth. This paper also proposes two new classes of a CPS bandpass filter using the resonators. CPS resonators are realized with open- and short-ended strips in various configurations, and lumped-element equivalent circuits for the resonators and CPS bandpass filters are presented. The proposed CPS bandpass filters have low insertion losses at passband and wide suppression bandwidths at stopbands.

A wide-band CPS-to-microstrip transition is presented and used for the measurements. With the aid of the transition, convenient CPS measurements can be accomplished with a conventional microstrip line. The back-to-back transition has an insertion loss of less than 3 dB and a return loss of better than 10 dB for the frequency range from 1.3 to 13.3 GHz (1 : 10.2).

Most of the modeling is based on electromagnetic approach. The circuit simulations were performed with the aid of IE3D software,[1] which uses the method-of-moment algorithm for full-wave electromagnetic simulation. The measured results agree very well with simulated data.

II. CPS Characteristics Analysis for the Design Consideration

The structure of CPS on the finite substrate is illustrated in Fig. 1. Strip width (W) and separation between the strips (s) are 1.5 and 0.6 mm, respectively, for all the presented circuits in this paper. All the circuits are fabricated on the RT/Duroid 5870 substrate with 1-oz copper, 20-mil substrate height, and the dielectric constant of 2.33.

[1]IE3D version 8, Zeland Software Inc., Fremont, CA, Jan. 2001.

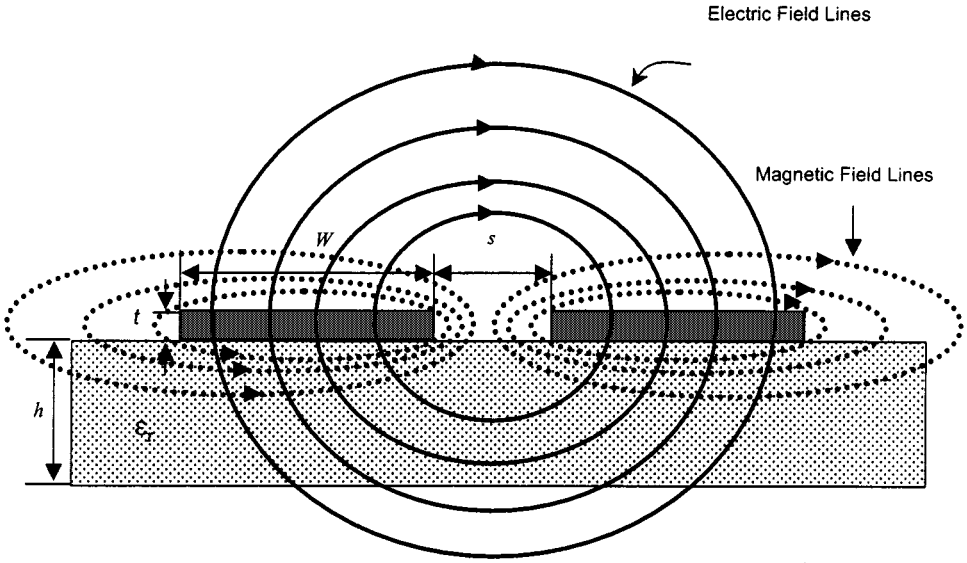

Fig. 1. CPS structure.

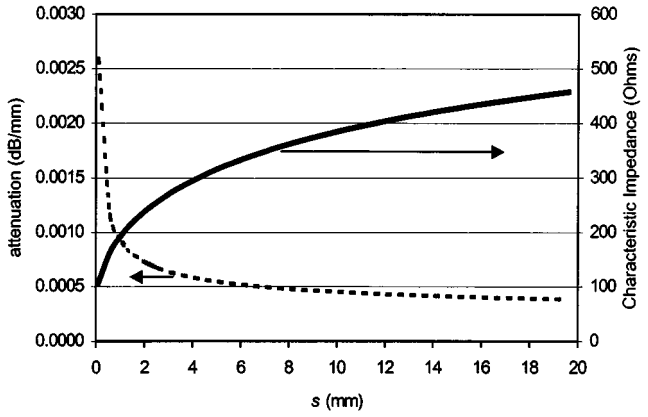

Fig. 2. Total attenuation $(\alpha_c + \alpha_d)$ as a function of separation width (s) at 10 GHz. The strip width is fixed ($W = 1.5$ mm).

Analytical techniques for calculating the characteristic impedance, effective dielectric constant, and dielectric and conductor losses of the CPS are well described in [7]–[9]. Closed-form quasi-TEM parameters for the symmetric CPS on the finite substrate thickness are necessary for the practical purpose, which is extensively discussed in [18].

Loss mechanisms considered in this paper are conductor (α_c) and dielectric (α_d) losses. Total attenuation including dielectric and conductor losses at 10 GHz is plotted in Fig. 2 with a fixed strip width ($W = 1.5$ mm) and separation between the strips (s) changed from 0.1 to 20 mm. It is observed that the wider the separation (s), the lower the total attenuation $(\alpha_c + \alpha_d)$ and the higher the characteristic impedance (Z_0) achieved. In other words, the higher the characteristic impedance of CPS, the lower the transmission-line attenuation achieved. The relationship between the dielectric constant of the substrate and the total attenuation is the higher the dielectric constant, the higher the total attenuation. For a practical design, moderate characteristic impedance with a proper dielectric constant substrate is used for low attenuation. Hence, Fig. 2 is useful for selecting design parameters.

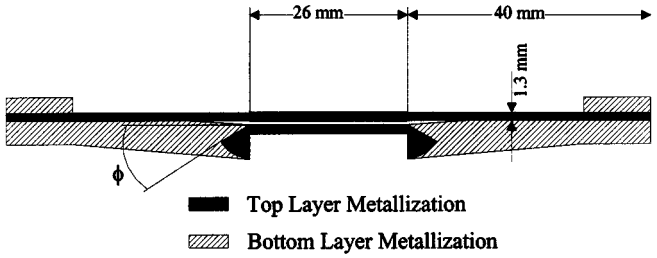

Fig. 3. Microstrip-to-CPS-to-microstrip back-to-back transition structure.

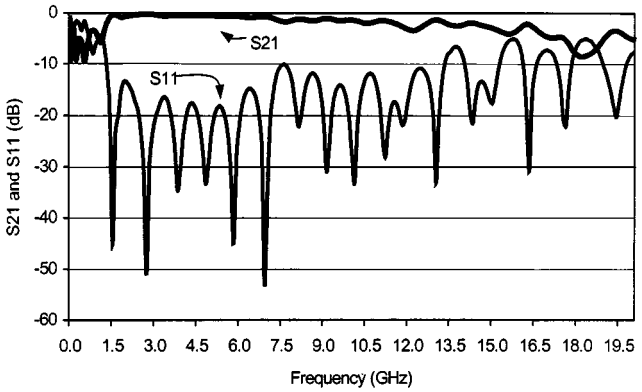

Fig. 4. Measured return and insertion loss of the back-to-back transition.

III. Microstrip-to-CPS-to-Microstrip Back-to-Back Transitions Developed for CPS Components Measurements

A wide-band microstrip-to-CPS-to-microstrip transition is developed, which operates from 1.3 to 13.3 GHz (1 : 10.2) with an insertion loss of less than 3 dB and a return loss of better than 10 dB for the back-to-back transition. The structure of back-to-back CPS-to-microstrip transitions is illustrated in Fig. 3 and the performance of developed transition is shown in Fig. 4.

This kind of CPS-to-microstrip transition, using a coupling method, was proposed by Simons *et al.* [19] in 1995 with

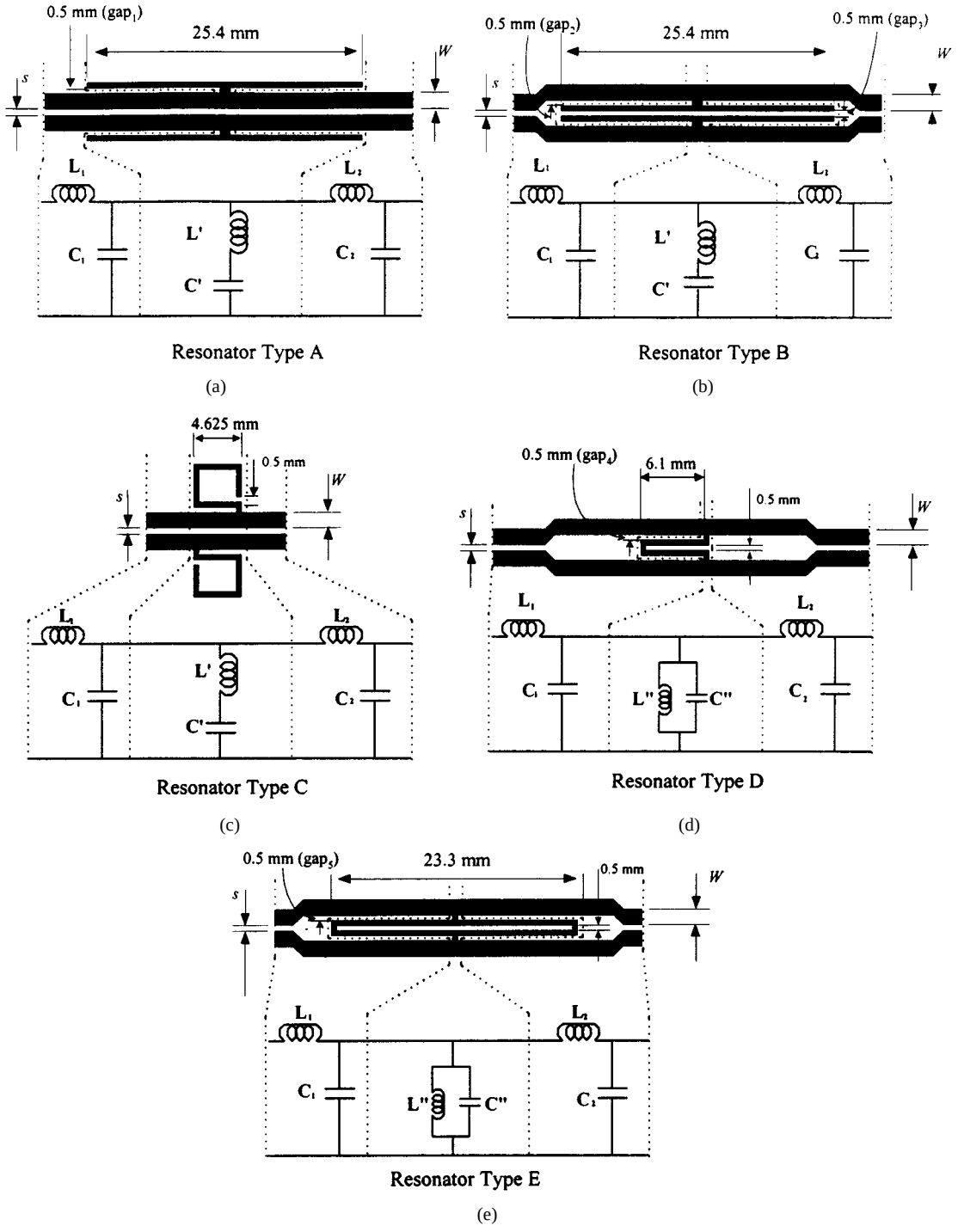

Fig. 5. Five basic types of CPS resonator with their lumped-element equivalent circuits.

an insertion loss of 2.4 dB over a bandwidth from 5.1 to 6.1 GHz (1 : 1.2) for a CPS-to-microstrip-to-CPS back-to-back transition.

The radial stub's radius is designed as 5.5 mm for broad-band operation. As shown in Fig. 1, electric-field lines of the CPS are distributed across the two strip lines and, on the contrary, electric-field lines of microstrip are directed normal to the substrate. Hence, the radial stub is rotated with an angle ϕ to change electric-field orientation from parallel to vertical to the substrate. The rotation angle ϕ is optimized as 30° for good coupling. The high characteristic impedance of CPS, i.e., 184 Ω, can be transformed to the microstrip line's 50 Ω by a smooth insertion of the ground plane toward the microstrip line. The width of microstrip line is optimized as 1.3 mm for the 50-Ω matching. Length of the microstrip line is chosen as 40 mm. Since it does not employ any quarter-wavelength transformers, which would limit the bandwidth, wide-band performance is achieved. All the following measurements are performed using this broad-band transition.

Though resonators and filters proposed in this paper require additional microstrip-to-CPS transitions for measurements, the transition affects comparably little to the frequency responses, and the insertion losses are deembedded by taking off the in-

TABLE I
LOADED Q (Q_L) AND UNLOADED Q (Q_u) OF THE RESONATOR TYPE A

gap_1 (mm)	s (mm)	Q_L	Q_u
0.25	0.6	113.6	114.7
	1.2	114.1	115.6
0.5	0.6	101.9	102.05
	1.2	104.7	105.2
1	0.6	62.6	72.8
	1.2	76.3	79.1

sertion losses of the transition and SMA connectors. In many applications, such as feeds to printed dipoles [1] and filters for rectennas [2]–[4], the CPS resonators and filters are integrated directly into the CPS circuit without using any transition.

IV. CPS RESONATORS DESIGN AND ANALYSIS

Fig. 5 illustrates five basic CPS resonators that use open- and short-ended strips with their lumped-element equivalent circuits. Combinations of these resonators can be used as variations. Types A–C use open-ended strips, and types D and E employ short-ended strips.

Resonator type A consists of open-ended T-strips with 0.5- mm width and around $\lambda_g/2$ (0.42 λ_g) or 25.4-mm length placed outside the strips designed to operate at the center frequency of near 4.28 GHz. As shown in Fig. 5, the CPS transmission line is represented as the lumped-element L–C circuits. The T-strips become inductor and the gap_1 induces coupling capacitance due to the coupling with CPS strips. Hence, T-strips can be represented as a shunt series resonator (L'–C' circuit), which acts as bandstop behavior. Narrow gap_1 creates high loaded $Q\,(Q_L)$ values due to the strong coupling and the low loss at the gap_1. As shown in Fig. 2, CPS transmission-line attenuation is reduced when the CPS strips separation (s) becomes wider. Correspondingly, narrower the gap_1 and wider the s will increase the loaded $Q\,(Q_L)$. Loaded (Q_L) and unloaded $Q\,(Q_u)$ values, simulated with IE3D, are displayed in Table I with various gap_1 and s values. Table I shows that the narrow gap_1 and the wide s configuration provides high Q_L value, and Q_u are almost identical to every configuration.

Q_u calculation of the bandstop resonator is described in [20] as follows:

$$Q_u = \frac{Q_L}{\sqrt{1 - 2 \times 10^{-L/10}}} \tag{1}$$

where Q_L is the loaded Q expressed as

$$Q_L = \frac{f_0}{\Delta f_{3\,\mathrm{dB}}}. \tag{2}$$

f_0, $\Delta f_{3\,\mathrm{dB}}$, and L represents the center frequency, 3-dB insertion loss bandwidth, and insertion loss at the center frequency, respectively.

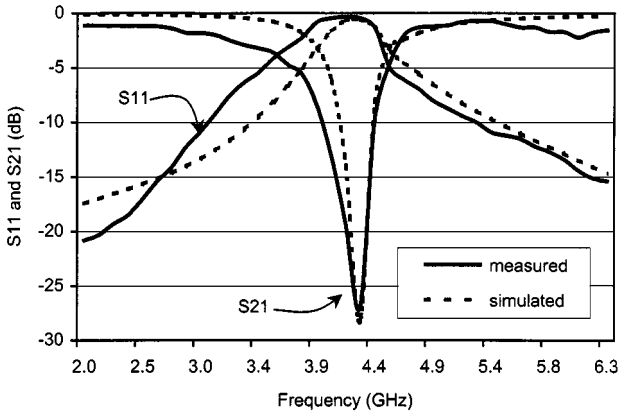

Fig. 6. Simulated and measured frequency responses for resonator type A.

TABLE II
LOADED Q (Q_L) AND UNLOADED Q (Q_u) OF THE RESONATOR TYPE B

gap_2 (mm)	gap_3 (mm)	Q_L	Q_u
0.25	0.5	127.2	129.1
	1.0	129.7	130.6
	2.0	136.1	137.4
0.5	0.5	121.25	121.27
	1.0	124.3	125.2
	2.0	134.3	134.9

Measured and simulated frequency responses of this type of resonator with 0.6 mm of s and 0.5 mm of the gap_1 are shown in Fig. 6. Measured Q_L of 97.27 is achieved with the resonance frequency of 4.28 GHz with the 3-dB insertion loss bandwidth of 44 MHz. Q_u of 97.44 is obtained from (1) with the insertion loss (L) of -27.53 dB at the center frequency. Measured Q values agree with simulated results ($Q_L = 101.9$ and $Q_u = 102.05$) displayed in Table I.

Resonator type B consists of open-ended T-strips placed inside of the CPS transmission line. The gap_2, the gap_3, and the open-ended T-strip's width are all 0.5 mm. To place the open-ended T-strips between the narrowly spaced CPS strips, the transmission line is widened from 0.6 to 2.5 mm, which corresponds to the impedance value changed from 184 to 250 Ω. Though the impedance changed, little insertion loss deterioration occurs and the return-loss response is better than 10 dB. The open-ended T-strip's length is around $\lambda_g/2$ (0.39 λ_g) or 25.4 mm at the center frequency of near 4.02 GHz. This type of resonator, similar to type A, has also coupling capacitance at the gap_2, and additional capacitance takes place at the gap_3. Table II describes the simulated Q values of the resonator type B with various gap_2 and s values. The narrower the gap_2 and the wider the s accomplishes higher Q_L values due to the stronger coupling capacitance and the lower transmission-line attenuation, as shown in Fig. 2. It can be said that the higher characteristic impedance corresponds to the higher Q_L values for CPS resonators, as shown in Tables I, II, and Fig. 2.

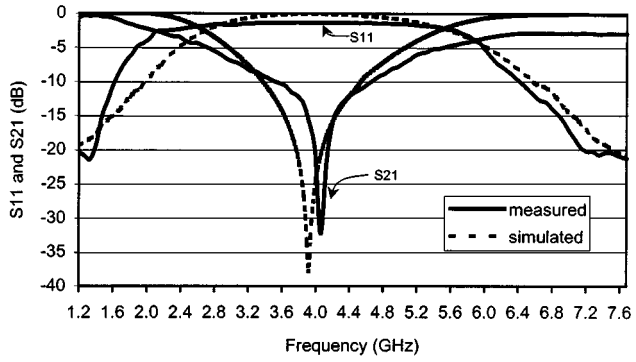

Fig. 7. Simulated and measured frequency responses for resonator type B.

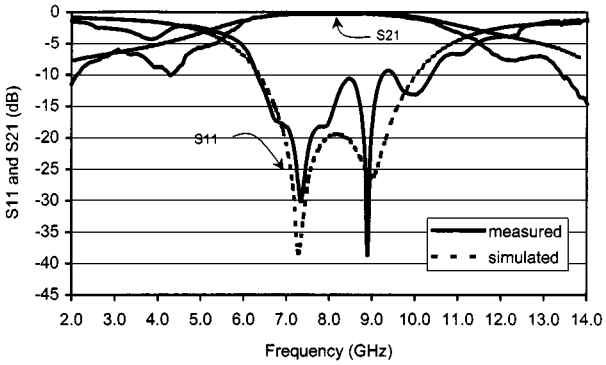

Fig. 9. Simulated and measured frequency responses for resonator type D.

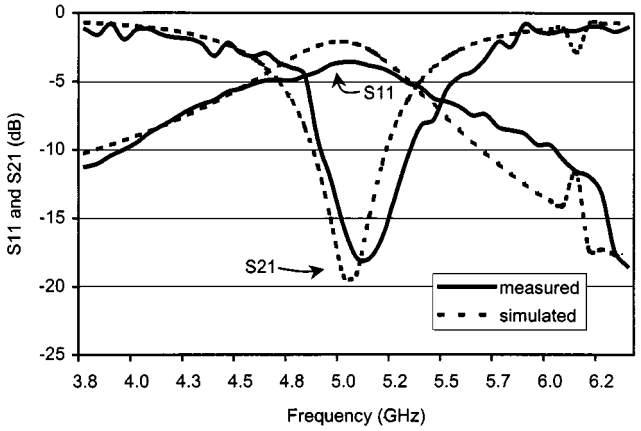

Fig. 8. Simulated and measured frequency responses for resonator type C.

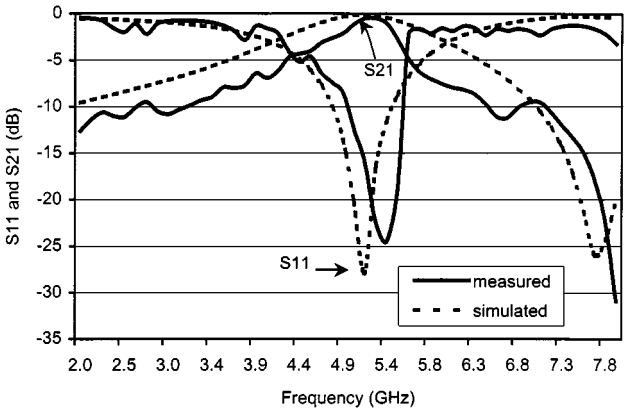

Fig. 10. Simulated and measured frequency responses for resonator type E.

Simulated and measured frequency responses of the type B resonator are shown in Fig. 7. Measured Q_L and Q_u values of the resonator type B, with 0.5 mm of gap_2 and gap_3 are 98.04 and 98.09, respectively. The 3-dB insertion loss bandwidth is 41 MHz and the insertion loss (L) is -32.22 dB at the center frequency. The simulated Q_L and Q_u values are 121.25 and 121.27, respectively, given in Table II.

Resonator type C has two open-ended strips located outside of the strips, which is similar to type A. These open-ended strips are bent to have square forms. The length of the open-ended strip is approximately 0.32 λ_g (15.52 mm) at the center frequency of near 5.08 GHz. This resonator has a shorter coupling arm (4.625 mm) than that of types A and B. Therefore, the open-ended strips have loose coupling and induce high losses. Two open-ended strips are purposely located asymmetrically to prevent any possible radiation as the dipole antenna does. The asymmetric structure induces spurious response around 6.1 GHz. Measured and simulated return and insertion losses of this resonator are described in Fig. 8. Measured Q_L and Q_u of this resonator are 23.51 and 23.87, respectively. The 3-dB insertion loss bandwidth is 216 MHz and the insertion loss (L) is -18.3 dB at the center frequency. Simulated Q_L and Q_u are 38.1 and 38.51, respectively.

Resonator type D utilizes a short-ended strip, in contrast to resonators types A–C. One of the merits of a uniplanar transmission line is convenient implementation of the short-ended strips without any via-holes. The total length of the short-ended strip is approximately 0.44 λ_g (13.7 mm), which is around $\lambda_g/2$, with 0.5-mm width at the center frequency of near 8 GHz. The transmission line is widened (the same as the resonator type B) to place the short-ended strip between the CPS strips, but little insertion-loss deterioration occurs and return loss is better than 10 dB. The short-ended strip becomes the inductor and the gap_4 induces coupling capacitance due to the coupling with CPS strips. This short-ended strip and gap_4 consist of a shunt parallel resonator (L''–C'' circuit), which act as bandpass behavior. Measured and simulated frequency responses of this resonator are well described in Fig. 9. Measured insertion loss of 0.12 dB is achieved at the center frequency of 8.12 GHz. This kind of resonator can be utilized for bandpass filter applications. Measured bandwidth of less than 3-dB insertion loss and better than 10-dB return loss is around 3 GHz (36.94%) with the resonator type D.

For the resonator type E, two short-ended strips are attached together with a shape of a closed polygon. Similar to the type D resonator, coupling capacitance at the gap_5 and short-ended strip's inductance consist of a shunt parallel resonator (L''–C'' circuit), which has bandstop behavior. The total length of the short-ended strip is approximately 1.1 λ_g (48.1 mm) at the center frequency of near 5.4 GHz. The transmission line is widened the same as resonators types B and D. Frequency responses of this resonator are illustrated in Fig. 10. Measured bandwidth of less than 3-dB insertion loss and better than 10-dB return loss is approximately 0.84 GHz (15.67%). Measured insertion loss of 0.5 dB was achieved at the center frequency of 5.36 GHz. Compared to resonator type D, bandwidth of

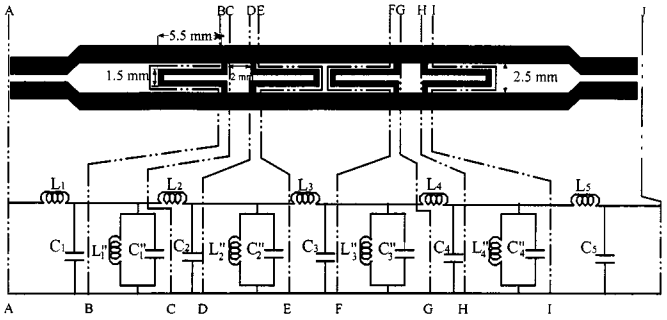

Fig. 11. Bandpass filter structure using multiple short-ended strips and lumped-element equivalent circuit.

resonator type E is almost one-half of that of resonator type C, which is due to the cascading of two identical resonators.

Five different types of resonators are presented and their performances are analyzed. As discussed, resonator type B has the highest Q_L among the three different open-ended strip resonators, and resonator type D has the widest bandwidth between the two different short-ended strip resonators.

From Tables I, II, and Fig. 2, CPS resonators can have high Q_L when high characteristic impedance and strong coupling capacitance takes place. It is possible to have many variations and combinations of these five resonators. Therefore, they would be very useful for designing CPS components such as filters.

V. CPS Bandpass Filters Realization With Presented Resonators

This section describes two new classes of CPS bandpass filters, which utilize combinations of the presented resonators. These bandpass filters have good passband insertion loss and wide-stopband suppressions. All the measurements were performed with the CPS-to-microstrip transition circuit presented in Section III.

A. Bandpass Filter Realization Using Multiple Short-Ended Strips

This type of bandpass filter uses the type D resonators presented in Section IV. The structure and lumped-element equivalent circuit of this filter are shown in Fig. 11. A transmission line with periodically loaded reactive cells has the characteristic of filters [21]. One reactive cell can be formed with the resonator type D, which has the bandstop behavior. The total length of the unit cell is around $\lambda_g/2$ (0.41 λ_g) or 12.5 mm at the center frequency of 8 GHz. The spacing between the neighboring cell is one of the important factors for bandpass filter design in periodic structure. Due to the structural dimension of the unit cell, it is impossible to have even spacing between unit cells. Hence, two neighboring cells are grouped as a sub-cell. Correspondingly, this bandpass filter has two sub-cells. Within a sub-cell, the spacing between the unit cells is optimized as 2 mm. The spacing shorter than 2 mm between unit cells has loose band rejection at stopbands. The spacing longer than 2 mm between unit cells has sharper band rejection, but has unsatisfactory return loss at passband. A distance between sub-cells is approximately $\lambda_g/2$ (0.46 λ_g) or 14 mm to have a good rejection at stopbands similar to a conventional periodic

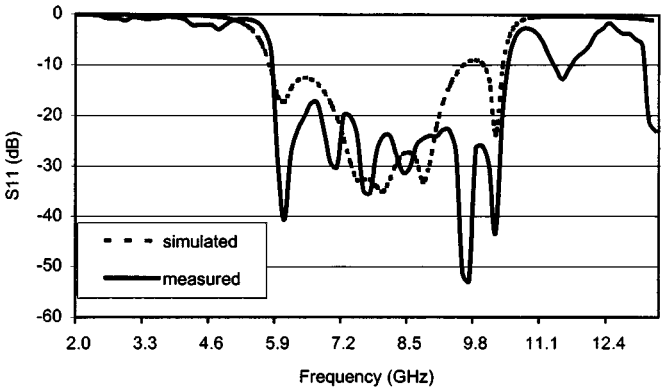

(a)

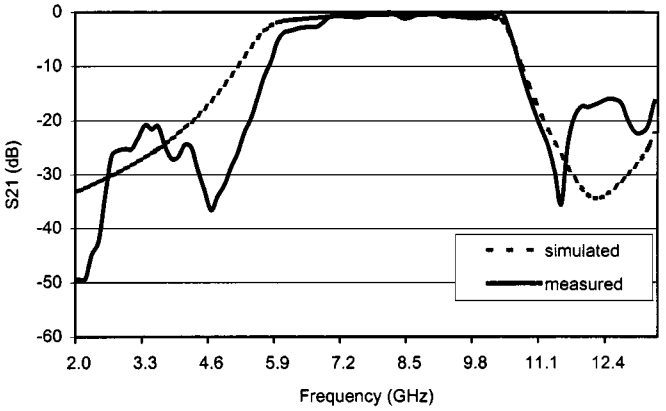

(b)

Fig. 12. Simulated and measured frequency responses of the bandpass filter using multiple short-ended strips. (a) Return loss. (b) Insertion loss.

structure [21]. As shown in Fig. 11, CPS transmission-line sections are represented as the lumped-element L–C circuits. The short-ended strip consists of a shunt parallel resonator (L''–C'' circuits), discussed in Section IV, for resonator type D. The transmission line is widened the same as the resonator types B, D, and E. For designing CPS components, the transmission line's inductance and capacitance values play important factors and should be considered for CPS components modeling. Values of the capacitance and inductance of CPS strips can be accurately extracted by employing IE3D's lumped-element extraction method. Simulated and measured frequency responses of this filter are illustrated in Fig. 12. Measured insertion loss of 0.48 dB is achieved at the center frequency of 8.24 GHz. A wide bandwidth of 4.16 GHz (52%) is achieved with less than 3-dB insertion loss and better than 10-dB return loss, and the 1-dB insertion-loss bandwidth is from 6.9 to 9.8 GHz. Stopbands range from 2 to 5.38 GHz at lower band area and from 11.1 to 13.31 GHz at higher band area.

B. Bandpass Filter Using Short-Ended Strips With T-Strips

Fig. 13 illustrates the bandpass filter structure using short-ended strips with T-strips and shows its lumped-element equivalent circuit. This type of filter consists of type A, E resonators and interdigital capacitors. Short-ended strips (type E resonators) are represented as shunt parallel resonators (L''–C'' circuits) and T-strips (type A resonators) are represented as a

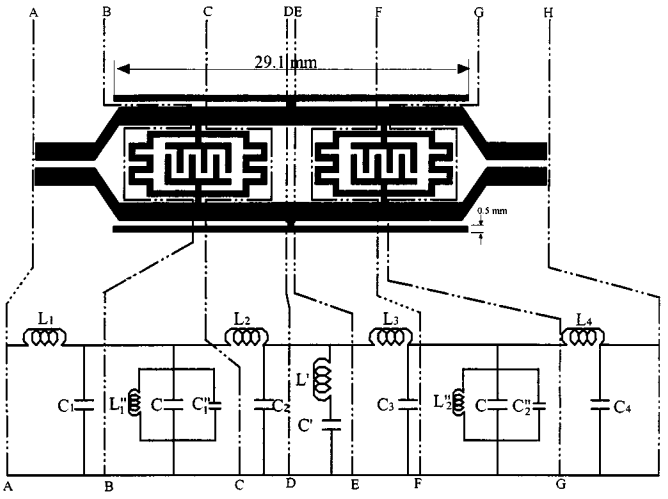

Fig. 13. Structure of the bandpass filter using short-ended strips with T-strips and its lumped-element equivalent circuit.

shunt series resonator (L'–C' circuit). An interdigital capacitor (C) is placed inside each type E resonator to give a bigger capacitance. The interdigital capacitor is widely used as the microwave circuit's lumped-element component possessing tight coupling. Analysis of the interdigital capacitor is well described in [22]. The number and length of the interdigital capacitor's fingers are $N = 3$ and 2 mm, respectively. All the gap distances of interdigital capacitors are uniformly 0.5-mm apart, which has the capacitance (C) of approximately 0.31 pF. Most of the capacitance takes place at the edges of the fingers. Hence, the gap distance between fingers together with the number of fingers is an important factor to determine the capacitance value.

The width of the short-ended strip is 0.5 mm with the length of 0.79 λ_g or 41.5 mm. The capacitance (C'') and inductance (L'') values of the short-ended strip are approximately 0.00563 pF/mm and 0.0763 nH/mm at 5 GHz, which can be found by IE3D software. The inductance (L'') and total capacitance including interdigital capacitance ($C_T = C + C''$) can be found by the following equations:

$$L'' = 0.0463 \times l \text{ nH} \tag{3}$$

$$C_T = 0.31 + 0.00563 \times l \text{ pF} \tag{4}$$

where l is the total length of the short-ended strip in millimeters. With (3) and (4), the approximate dimension of the short-ended strip can be found at the desired frequency.

Two unit cells are cascaded with the distance of around $\lambda_g/4$ (0.28 λ_g) or 13.6 mm. The type A resonator (L'–C' circuit) is combined with this filter to enhance the suppression at the lower stopband with the length of 29.1 mm (0.48 λ_g) at the center frequency of near 4 GHz. This is a good example of the uniplanar transmission-line's benefit that can have open- and short-ended strips together without any via holes. Measured bandwidth of less than 1-dB insertion loss and better than 10-dB return loss ranges from 4.82 to 5 GHz (3.64%). Stopbands with the suppression of less than 20-dB range from 3.56 to 3.98 GHz (0.42 GHz)

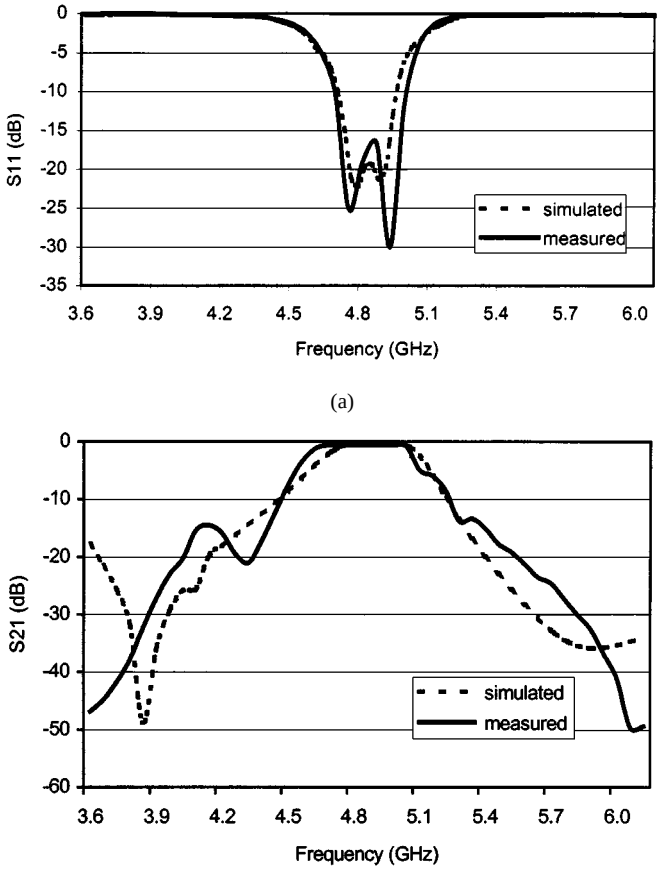

Fig. 14. Simulated and measured frequency responses of the bandpass filter using short-ended strips with T-strips. (a) Return loss. (b) Insertion loss.

at lower band and from 5.48 to 6.08 GHz (0.6 GHz) at higher band. Low insertion loss of 0.61 dB was measured at the center frequency of 4.94 GHz. Measured and simulated frequency responses are given in Fig. 14, which shows good agreement between the measured and simulated data.

VI. Conclusions

Five types of CPS resonators have been presented and their performances analyzed. CPS characteristics are analyzed for the circuit design consideration. For the demonstrations of these resonators' applications, two new classes of bandpass filters are designed and tested. Measurement results show low-passband insertion losses and good stopband suppressions. For conducting the measurements, a wide-band microstrip-to-CPS-to-microstrip back-to-back transition is developed and used. Less than 3-dB insertion loss and better than 10-dB return-loss bandwidth is achieved from 1.3 to 13.3 GHz for the back-to-back transition. Simulated and measured data have good agreements.

The resonators and bandpass filters should find wide applications for uniplanar circuit implementation.

Acknowledgment

The authors would like to thank C. Wang, Texas A&M University, College Station, for technical assistance.

REFERENCES

[1] K. Tilley, X. D. Wu, and K. Chang, "Coplanar waveguide fed coplanar strip dipole antenna," *Electron. Lett.*, vol. 30, no. 3, pp. 176–177, Feb. 1994.

[2] J. O. McSpadden, T. Yoo, and K. Chang, "Theoretical and experimental investigation of a rectenna element for microwave power transmission," *IEEE Trans. Microwave Theory Tech.*, vol. 40, pp. 2359–2366, Dec. 1992.

[3] T. Yoo and K. Chang, "Theoretical and experimental development of 10 and 35 GHz rectennas," *IEEE Trans. Microwave Theory Tech.*, vol. 40, pp. 1259–1266, June 1992.

[4] J. O. McSpadden, L. Fan, and K. Chang, "Design and experiments of a high-conversion-efficiency 5.8-GHz rectenna," *IEEE Trans. Microwave Theory Tech.*, vol. 46, pp. 2053–2060, Dec. 1998.

[5] H. K. Chiou, C. Y. Chang, and H. H. Lin, "Balun design for uniplanar broad band double balanced mixer," *Electron. Lett.*, vol. 31, no. 24, pp. 2113–2114, Nov. 1995.

[6] J. H. Son, H. H. Wang, J. F. Whitaker, and G. A. Mourou, "Picosecond pulse propagation on coplanar striplines fabricated on lossy semiconductor substrates: Modeling and experiments," *IEEE Trans. Microwave Theory Tech.*, vol. 41, pp. 1574–1580, Sept. 1993.

[7] G. Ghione, "A CAD-oriented analytical model for the losses of general asymmetric coplanar lines in hybrid and monolithic MICs," *IEEE Trans. Microwave Theory Tech.*, vol. 41, pp. 1499–1510, Sept. 1993.

[8] E. Chen and S. Y. Chou, "Characteristics of coplanar transmission lines on multilayer substrates: Modeling and experiments," *IEEE Trans. Microwave Theory Tech.*, vol. 45, pp. 939–945, June 1997.

[9] Z. Du, K. Gong, J. S. Fu, Z. Feng, and B. Gao, "CAD model for asymmetrical, elliptical, cylindrical, and elliptical cone coplanar striplines," *IEEE Trans. Microwave Theory Tech.*, vol. 48, pp. 312–316, Feb. 2000.

[10] R. N. Simons, N. I. Dib, and L. P. B. Katehi, "Modeling of coplanar stripline discontinuities," *IEEE Trans. Microwave Theory Tech.*, vol. 44, pp. 711–716, May 1996.

[11] K. Goverdhanam, R. N. Simons, and L. P. B. Katehi, "Coplanar stripline components for high-frequency applications," *IEEE Trans. Microwave Theory Tech.*, vol. 45, pp. 1725–1729, Oct. 1997.

[12] ——, "Coplanar stripline propagation characteristics and bandpass filter," *IEEE Microwave Guided Wave Lett.*, vol. 7, pp. 214–216, Aug. 1997.

[13] S. G. Mao, H. K. Chiou, and C. H. Chen, "Modeling of lumped-element coplanar-stripline low-pass filter," *IEEE Microwave Guided Wave Lett.*, vol. 8, pp. 141–143, Mar. 1998.

[14] S. Uysal and J. W. P. Ng, "A compact coplanar stripline lowpass filter," in *Asia–Pacific Microwave Conf.*, vol. 2, 1999, pp. 307–310.

[15] N. Dib, L. Katehi, G. Ponchak, and R. Simons, "Theoretical and experimental characterization of coplanar waveguide discontinuities for filter applications," *IEEE Trans. Microwave Theory Tech.*, vol. 39, pp. 873–882, May 1991.

[16] K. Hettak, N. Dib, A. Sheta, and S. Toutain, "A class of novel uniplanar series resonators and their implementation in original applications," *IEEE Trans. Microwave Theory Tech.*, vol. 46, pp. 1270–1276, Sept. 1998.

[17] K. Hettak, N. Dib, A. Omar, G. Delisle, M. Stubbs, and S. Toutain, "A useful new class of miniature CPW shunt stubs and its impact on millimeter wave integrated circuits," *IEEE Trans. Microwave Theory Tech.*, vol. 47, pp. 2340–2349, Dec. 1999.

[18] K. C. Gupta, R. Grag, I. Bhal, and P. Bhartia, *Microstrip Lines and Slotlines*, 2nd ed. Norwood, MA: Artech House, 1996.

[19] R. N. Simons, N. I. Dib, and L. P. B. Katehi, "Coplanar stripline to microstrip transition," *Electron. Lett.*, vol. 31, no. 20, pp. 1725–1726, Sept. 1995.

[20] J. Caroll, M. Li, and K. Chang, "New technique to measure transmission line attenuation," *IEEE Trans. Microwave Theory Tech.*, vol. 43, pp. 219–222, Jan. 1995.

[21] D. M. Pozar, *Microwave Engineering*, 2nd ed. New York: Wiley, 1998.

[22] F. Huang, B. Avenhaus, and M. J. Lancaster, "Lumped-element switchable superconducting filters," *Proc. Inst. Elect. Eng.*, pt. H, vol. 146, pp. 229–233, June 1999.

Young-Ho Suh (S'01) received the B.S degree in electrical and control engineering from the Hong-Ik University, Seoul, Korea, in 1992, the M.S degree in electrical engineering from Texas A&M University, College Station, in 1998, and is currently working toward the Ph.D. degree at Texas A&M University.

From 1992 to 1996, he was a Research Engineer with the LG-Honeywell Corporation Ltd., Seoul, Korea. From 1996 to 1998, he was involved with the development of robust wireless communication systems for a GSM receiver under a multipath fading channel. He is current a Research Assistant with the Electromagnetics and Microwave Laboratory, Texas A&M University. His research interests includes uniplanar transmission-line analysis and components development, microwave power transmission, antennas for wireless communications, and microwave integrated circuits.

Kai Chang (S'75–M'76–SM'85–F'91) received the B.S.E.E. degree from the National Taiwan University, Taipei, Taiwan, R.O.C., in 1970, the M.S. degree from the State University of New York at Stony Brook, in 1972, and the Ph.D. degree from The University of Michigan at Ann Arbor, in 1976.

From 1972 to 1976, he was with the Microwave Solid-State Circuits Group, Cooley Electronics Laboratory, The University of Michigan at Ann Arbor, where he was a Research Assistant. From 1976 to 1978, he was with Shared Applications Inc., Ann Arbor, MI, where he was involved with computer simulation of microwave circuits and microwave tubes. From 1978 to 1981, he was with the Electron Dynamics Division, Hughes Aircraft Company, Torrance, CA, where he was involved in the research and development of millimeter-wave solid-state devices and circuits, power combiners, oscillators, and transmitters. From 1981 to 1985, he was with TRW Electronics and Defense, Redondo Beach, CA, where he was a Section Head involved with the development of state-of-the-art millimeter-wave integrated circuits and subsystems, including mixers, voltage-controlled oscillators (VCOs), transmitters, amplifiers, modulators, upconverters, switches, multipliers, receivers, and transceivers. In August 1985, he joined the Electrical Engineering Department, Texas A&M University, College Station, as an Associate Professor, and became a Professor in 1988. In January 1990, he became an E-Systems Endowed Professor of Electrical Engineering. He has authored and co-authored several books, including *Microwave Solid-State Circuits and Applications* (New York: Wiley, 1994), *Microwave Ring Circuits and Antennas* (New York: Wiley, 1996), *Integrated Active Antennas and Spatial Power Combining* (New York: Wiley, 1996), and *RF and Microwave Wireless Systems* (New York: Wiley, 2000). He has served as the Editor of the four-volume *Handbook of Microwave and Optical Components* (New York: Wiley, 1989 and 1990). He is the Editor of *Microwave and Optical Technology Letters* and the Wiley Book Series on "Microwave and Optical Engineering." He has also authored or co-authored over 350 technical papers and several book chapters in the areas of microwave and millimeter-wave devices, circuits, and antennas. His current interests are in microwave and millimeter-wave devices and circuits, microwave integrated circuits, integrated antennas, wide-band and active antennas, phased arrays, microwave power transmission, and microwave optical interactions.

Dr. Chang was the recipient of the 1984 Special Achievement Award presented by TRW, the 1988 Halliburton Professor Award, the 1989 Distinguished Teaching Award, the 1992 Distinguished Research Award, and the 1996 Texas Engineering Experiment Station (TEES) Fellow Award presented by Texas A&M University.